Journal of Translational Regenerative Medicine

2026. Volume 1

Research Paper

Continuous Extrusion-based 3D Printing of a Compositionally Differentiated Hydrogel Scaffold for Regenerative Endodontics: A Feasibility Study

Mohammad Ali Ketabi[1], Arezoo Mirzaiy[1], Mohammad Reza Khodadadzadeh Khaledi[1], MohammadHossein Shahrezaee[2, 3*], Ali Shakibaei Fard[1*]

1. Department of Endodontics, Faculty of Dentistry, AJA University of Medical Sciences, Tehran, Iran.
2. School of Dentistry, Tehran University of Medical science, Tehran, Iran.
3. Department of Oral and Maxillofacial Surgery, TM.C., Islamic Azad University, Tehran, Iran.

Use your device to scan and read the article online

Citation Ketabi MA, Mirzaiy A, Khodadadzadeh Khaledi MR, Shahrezaee M, Shakibaei Fard A. Continuous Extrusion-based 3D Printing of a Compositionally Differentiated Hydrogel Scaffold for Regenerative Endodontics: A Feasibility Study. Journal of Translational Regenerative Medicine. 2026; 1:E1024. http://dx.doi.org/10.32598/JTRM.1.1024

http://dx.doi.org/10.32598/JTRM.1.1024

ABSTRACT

Background: Pulp necrosis in immature permanent teeth halts root development, producing thin dentinal walls and increasing fracture risk. Conventional apexification can create an apical barrier but does not reliably support continued root maturation. This study aimed to fabricate a two-region hydrogel scaffold using continuous extrusion-based three-dimensional (3D) printing and assess it with cone-beam computed tomography (CBCT).

Methods: This is a laboratory feasibility study. A simulated immature root canal was prepared in an extracted human tooth and assessed using CBCT. The measured root length and minimum canal diameter served as anatomical references for scaffold dimensions. The scaffold consisted of an alginate–carboxymethyl chitosan (CMC) region and an alginate- nominal 45S5 bioactive glass region. Both formulations were sequentially loaded into a single cartridge and extruded through one nozzle without post-printing assembly. Six fabrication attempts were made, of which 5 attempts met the operational criteria of full layer deposition, preserved gross configuration, and visible continuity between regions. Therefore, five completed scaffolds underwent qualitative macroscopic evaluation during printing, crosslinking, washing, handling, and biopsypunch preparation.

Results: The constructs displayed two distinguishable yet continuous material regions. No gaps, fragmentation, delamination, collapse, or separation were observed after crosslinking, washing, or preparation of 50 punched specimens (2–5 mm diameter).

Conclusion: Continuous extrusion through one cartridge and nozzle enables fabrication of a compositionally differentiated two-region hydrogel scaffold with preserved macroscopic continuity. Further quantitative architectural, mechanical, degradation, and biological evaluations are required to determine functional significance.

Keywords: Regenerative endodontics, Hydrogel scaffold, Three-dimensional (3D) bioprinting, Continuous extrusion, Cone-beam computed tomography (CBCT)

Article info:
Received: 21 Jul 2026
Accepted: 12 Nov 2026
Publish: 25 Dec 2026

*** Corresponding Author:**
Ali Shakibaei Fard, DDS.
Address: *Department of Endodontics, Faculty of Dentistry, AJA University of Medical Sciences, Tehran, Iran.*
E-mail: *Aaallliiish7731@gmail.com*

Highlights

- Two hydrogel scaffold formulations were deposited sequentially through one cartridge and nozzle.
- The two regions differed in composition but shared the same nominal printing architecture.
- Five of six fabrication attempts produced completed 20-layer constructs.
- Completed scaffolds maintained gross continuity during crosslinking, washing, and punching.
- CBCT informed scaffold scale but did not demonstrate canal adaptation.

Plain Language Summary

Pulp necrosis in an immature permanent tooth can interrupt normal root development. The resulting short roots and thin root walls may make the tooth more susceptible to fracture. Existing treatments can help form a barrier at the root tip, but they do not necessarily restore normal root development. Researchers are therefore investigating materials and methods that might support future regenerative approaches. In this laboratory study, we investigated whether a continuous, soft, water-based scaffold with two different material compositions could be made using three-dimensional (3D) printing. A scaffold is a temporary structure that may provide a physical environment for future tissue formation. One material mixture contained alginate and carboxymethyl chitosan; the other contained alginate and a glass-based material. The mixtures were loaded sequentially into the same printer cartridge and extruded through a single nozzle, producing one continuous structure with two distinct regions. Five of the six printing attempts produced complete scaffolds. These scaffolds remained visibly intact and continuous during calcium chloride treatment, washing, handling, and preparation of 50 smaller specimens. The findings show that this printing method can produce a scaffold with two material compositions without printing the regions separately and joining them afterward. This study assessed only whether the scaffolds could be printed and handled. It did not evaluate their mechanical strength, degradation, internal structure, biological effects, or fit within a root canal. Further research is needed before their potential use in regenerative dental treatment can be assessed.

Introduction

Management of pulp necrosis in immature permanent teeth with open apices remains a significant clinical challenge. Loss of pulp vitality interrupts continued root development, resulting in short roots with thin dentinal walls and increased susceptibility to fracture [1-3]. Conventional approaches, including calcium hydroxide apexification and mineral trioxide aggregate apical plug placement, can promote formation of an apical barrier; however, they do not predictably promote continued root elongation or dentinal wall thickening [1-3].

Tissue-engineered scaffolds provide a potential platform for regenerative endodontic strategies by offering a three-dimensional (3D) environment for tissue formation. Conventional scaffold-fabrication techniques may provide limited control over geometry and reproducibility. In contrast, 3D printing can translate a digital design into a physical construct with predefined dimensions, filament orientation, and deposition path [4, 5]. Extrusion-based printing is particularly suitable for hydrogel fabrication because different formulations can be deposited sequentially during a single manufacturing process.

Cone-beam computed tomography (CBCT) provides 3D information regarding root canal morphology and can support ex vivo assessment of dental anatomy [6]. Even when quantitative scaffold-to-canal adaptation is not evaluated, CBCT-derived measurements may provide anatomical references for defining the scale of an experimental construct.

Regenerative endodontic procedures do not consistently reproduce an organized pulp-dentin complex [7-9]. A scaffold that incorporates spatial variation in material composition within a continuous construct may therefore provide a useful experimental platform for future regenerative investigations. Alginate and carboxymethyl chitosan (CMC) have been investigated as printable bio-

materials for dental tissue engineering, whereas 45S5 bioactive glass has been widely studied as a bioactive component of tissue-engineering composites [10-12]. Calcium-mediated ionic gelation is an established method for stabilizing alginate-containing hydrogels [13, 14].

The objective of this study was to fabricate a continuous two-region hydrogel scaffold using CBCT-derived anatomical measurements as references and continuous extrusion-based 3D printing, and to describe its macroscopic continuity after fabrication, crosslinking, washing, handling, and specimen preparation. The manufacturing concept examined in this study was the sequential deposition of two distinct hydrogel formulations through a single cartridge and nozzle, thereby creating compositional differentiation without separately printing and subsequently joining the two regions.

Materials and Methods

Study design and outcomes

This is a descriptive laboratory feasibility study. A human tooth extracted because of periodontal disease was used as the anatomical reference. The experimental unit for fabrication was one independently printed scaffold. Fabrication feasibility was evaluated across six independent printing attempts. For descriptive evaluation, a completed fabrication was operationally defined as deposition of the intended 20-layer construct with preservation of the gross scaffold configuration and visible continuity between the two material regions after printing. Subsequent handling feasibility was assessed by visual inspection for gross fragmentation, collapse, delamination, or separation during crosslinking, washing, handling, and biopsy-punch preparation. The study was not designed to compare punch diameters statistically or to quantify dimensional accuracy, pore architecture, interfacial strength, or mechanical performance.

Tooth preparation and cone-beam computed tomography imaging

After removal of residual soft tissue, the human tooth was stored in sterile 0.9% normal saline at 4 ˚C. Before experimental use, it was immersed in 5.25% sodium hypochlorite for 5 min and then thoroughly rinsed with sterile saline. The apical root region was manually modified to create a widened opening that macroscopically simulated an immature root with an open apex. The modified specimen was used as an experimental anatomical model rather than as a representation of a defined clinical stage of root development.

The modified tooth was scanned using CBCT. The images were stored in DICOM format and used for 3D reconstruction. The CBCT dataset was used only to derive overall anatomical measurements and to construct a resin representation of the simulated root anatomy. It was not used to validate dimensional accuracy or scaffold-to-canal fit (Figure 1).

Three-dimensional reconstruction and resin model

The DICOM dataset was imported into 3D Slicer v. 5.10.0. Threshold-based segmentation followed by manual refinement was used to isolate the tooth structure, remove visible artifacts, and obtain a 3D representation of the modified tooth. Because the study did not investigate segmentation accuracy, the reconstructed model was used as an anatomical reference rather than as a quantitatively validated replica.

The model was exported in STL format and fabricated with an Orange 4K DLP resin printer (LONGER, China) using Wanhao G125 resin. The nominal layer thickness was 0.05 mm and the exposure time was 3.2 s. The CBCT-derived root canal length was approximately 9-10 mm, and the smallest measured canal diameter was approximately 2 mm. These measurements informed the total scaffold height and the lower range of specimen diameters used during preparation. Direct seating of the hydrogel scaffold within the canal and quantitative assessment of fit were not performed (Figure 2).

Scaffold design

The scaffold was designed in Blender as a 20-layer construct composed of nominally rectangular deposited filaments arranged in alternating perpendicular directions. The nominal line width, interfilament spacing, and layer height were each set at 500 μm. These values represent design and printer-input parameters; the actual printed filament width and pore dimensions were not measured (Figure 3).

A total of 20 layers were selected to approximate the 9-10 mm root length derived from the anatomical model. The construct comprised two consecutive 10-layer regions. The same nominal printing architecture was applied to both regions; they differed only in material composition. Each printed scaffold had overall planar dimensions of approximately 4×4 cm, allowing multiple specimens to be obtained from each completed construct.

Preparation of the alginate-carboxymethyl chitosan formulation

For the first region, sodium alginate LV with extra pure (product No. 80726; Sisco Research Laboratories Pvt. Ltd., India) and CMC (product No. CMC029; Negin Sahand, Iran) were combined at a 1:1 mass ratio. The formulation contained 20% (w/v) sodium alginate and 20% (w/v) CMC, corresponding to a total polymer concentration of 40% (w/v). The polymers were dispersed in deionized water under continuous mechanical stirring until no grossly visible heterogeneity remained. Preliminary extrusion trials were used to establish practical handling and estimate the amount required for the corresponding layers.

Synthesis of nominal 45S5 bioactive glass

A glass powder with a nominal 45S5 composition of 45 wt% SiO_2, 24.5 wt% CaO, 24.5 wt% Na_2O, and 5 wt% P_2O_5 was synthesized using a sol-gel procedure adapted from a previous study [15]. Tetraethyl orthosilicate (16.6 mL) was added to 25 mL of deionized water and stirred for approximately 45 min, followed by adding 400 µL of 1 M nitric acid. After clarification of the solution, 1.44 mL of triethyl phosphate was incorporated and the mixture was stirred for a further 45 min. Calcium nitrate (10.33 g) was then added, followed by adding sodium nitrate (6.72 g) after 30-45 min.

The sol was maintained in a sealed container at room temperature for 3-5 days until gelation. The gel was dried at 70 ˚C for 48 h and at 120 ˚C for 24 h, followed by heat treatment at 700 ˚C for 3 h. The resulting material was ground using a planetary ball mill (Amin Asia, Iran) until a visually homogeneous fine powder was obtained. Particle-size distribution, phase composition, and final chemical composition were not independently quantified. Accordingly, the material was described as having a nominal 45S5 composition.

Preparation of the alginate-glass formulation

For the second region, sodium alginate was prepared at 20% (w/v). The nominal 45S5 glass powder was added at 20 wt% relative to the mass of sodium alginate; thus, 0.20 g of glass powder was used per gram of sodium alginate. The powder was gradually incorporated under continuous mechanical stirring until no grossly visible heterogeneity remained and the material could be extruded under the selected printing conditions.

Continuous sequential extrusion

Scaffolds were fabricated using an Aptin 3 extrusion-based bio-3D printer (Aptin Teb Fanavar Co., Iran) equipped with a stainless-steel cartridge and a 500-µm nozzle. The digital design was sliced using Slic3r. Printing was performed at room temperature at a nominal linear speed of 5 mm/s, nominal flow rate of approximately 1 mm^3/s, and nominal layer height of 500 µm. No independent rheological, pressure-based, or extrusion-fidelity characterization was performed.

The two formulations were prepared separately and loaded sequentially into the same cylindrical cartridge. The amount assigned to the first 10 layers was introduced and leveled first, followed by the amount assigned to the second 10 layers (Figure 4). During uninterrupted extrusion, the first formulation was deposited before the second formulation advanced through the same flow path. A visually apparent transition occurred between formulations. Its dimensions and composition were not quantified, and no post-printing bonding or assembly step was used.

Six independent scaffold-printing attempts were taken. All six attempts were retained in the descriptive fabrication count. Constructs meeting the operational completion criteria were carried forward for crosslinking, washing, and macroscopic handling assessment.

Crosslinking and washing

Immediately after printing, completed scaffolds were immersed in 20% (w/v) calcium chloride for 2 h at room temperature to ionically crosslink the alginate-containing formulations. The scaffolds were then washed three times with water at room temperature. The crosslinking conditions were treated as part of the fabrication protocol and were not evaluated as an independent variable.

Macroscopic evaluation and specimen preparation

Each completed scaffold was inspected visually after printing, crosslinking, washing, and handling. The assessment focused on gross fragmentation, collapse, delamination, visible gaps, and separation between the two material regions. Macroscopic continuity was defined as the absence of visible separation across the interface under routine handling.

Biopsy punches with diameters within the 2-5-mm range were used to obtain specimens from the completed scaffolds. A total of 10 punching procedures were

Table 1. Prespecified tooth design features and descriptive fabrication outcomes

Experimental Steps	Design or Procedure	Observed Outcome
Fabrication attempts	6 independent printing attempts	5 completed constructs
Scaffold configuration	20 layers; 2 consecutive 10-layer regions	Gross configuration preserved in completed constructs
Regional distinction	Different material formulations; same nominal printing architecture	2 visually distinguishable, continuous regions
Post-processing	Calcium chloride crosslinking and three washing cycles	No visible gap, gross fragmentation, collapse, delamination, or separation
Specimen preparation	10 punching procedures per completed scaffold; 50 total; punch range: 2-5 mm	No gross disruption or visible regional separation
Quantitative testing	Not performed	No inference regarding fit, pore architecture, strength, degradation, or biological function

performed per completed scaffold, yielding 50 punched specimens overall. Punch sizes were used for specimen preparation and were not treated as balanced comparative groups (Figure 5). Consequently, the study did not test a diameter-dependent effect. After punching, both the removed specimens and the remaining scaffold were inspected visually for gross disruption.

Data presentation

Fabrication outcomes were summarized descriptively as the number of completed attempts relative to the total number undertaken. Macroscopic observations were reported narratively. Punching procedures performed within the same scaffold were considered repeated handling observations rather than independent biological or mechanical replicates. No inferential statistical analysis was performed because the study did not generate quantitative comparative outcomes (Figure 6).

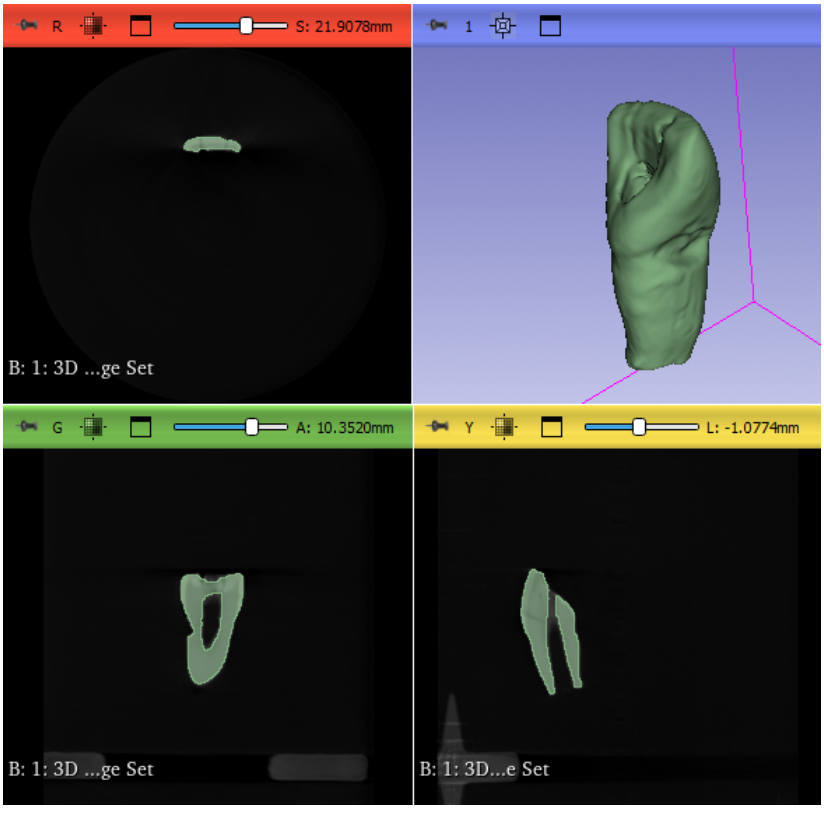

Figure 1. The 3D model of the modified tooth shown in three anatomical planes

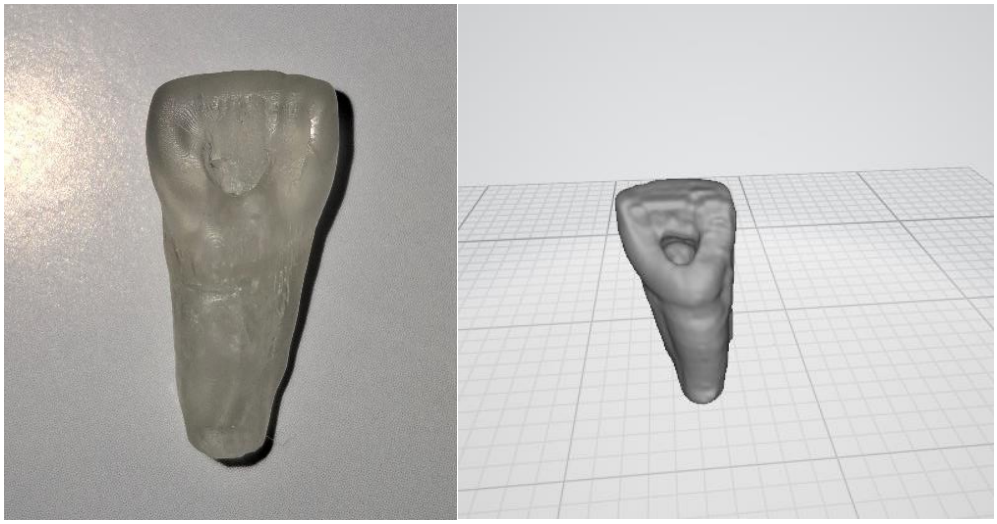

Figure 2. STL output of the tooth model (right) along with the resin-printed tooth model (left)

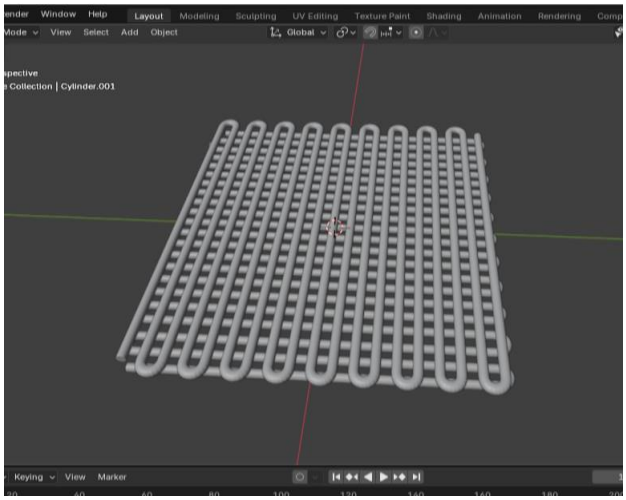

Figure 3. Schematic diagram of the designed scaffold

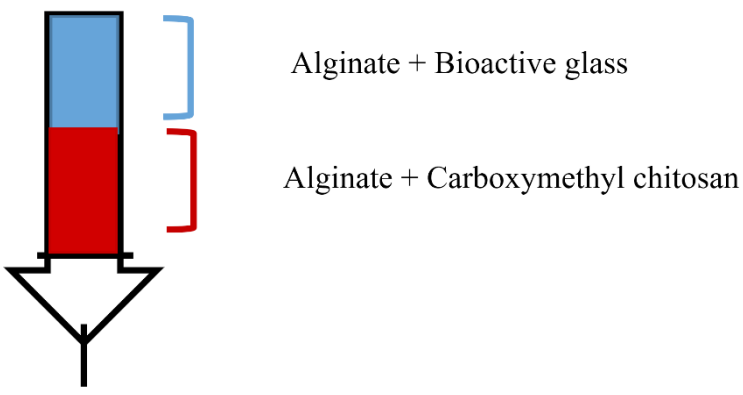

Figure 4. Schematic diagram of a cartridge containing two-phase ink content

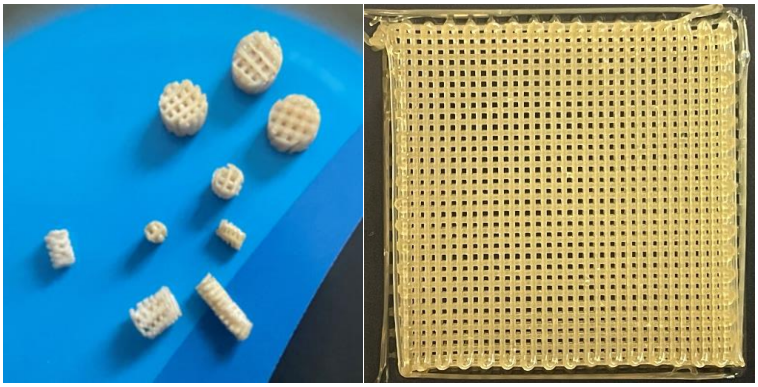

Figure 5. Extrusion-printed composite scaffold before and after punching in different sizes

Results

Fabrication feasibility

Among six independent fabrication attempts, five attempts met the operational completion criteria; one did not produce a completed construct and was not carried forward for downstream handling assessment. The five completed scaffolds preserved the intended gross 20-layer configuration and were suitable for crosslinking, washing, and specimen preparation (Table 1).

Macroscopic two-region continuity

The completed scaffolds contained two visually distinguishable material regions corresponding to the alginate-CMC and the alginate-glass formulations. Both regions shared the same nominal deposition architecture. A visually gradual transition was observed during sequential extrusion, although the dimensions and composition of this transition were not measured. After calcium chloride crosslinking and washing, no visible gap, gross fragmentation, collapse, delamination, or separation between the two regions was observed in the five completed scaffolds. The overall configuration remained intact during routine handling.

Macroscopic findings after punching

Ten punching procedures were performed on each of the five completed scaffolds (a total of 50 punched specimens) using punch diameters within the 2-5-mm range. Visual inspection of the removed specimens and remaining scaffold structures revealed no gross fragmentation, collapse, delamination, or visible separation between the two material regions. Because the punch diameters were not evaluated as balanced comparative groups, no conclusion was drawn regarding the effect of increasing punch diameter.

Discussion

This descriptive laboratory study demonstrated that two compositionally different hydrogel formulations could be deposited sequentially through one cartridge and nozzle to produce a continuous scaffold without a separate bonding step. Five of six fabrication attempts yielded completed constructs that remained macroscopically continuous after ionic crosslinking, washing,

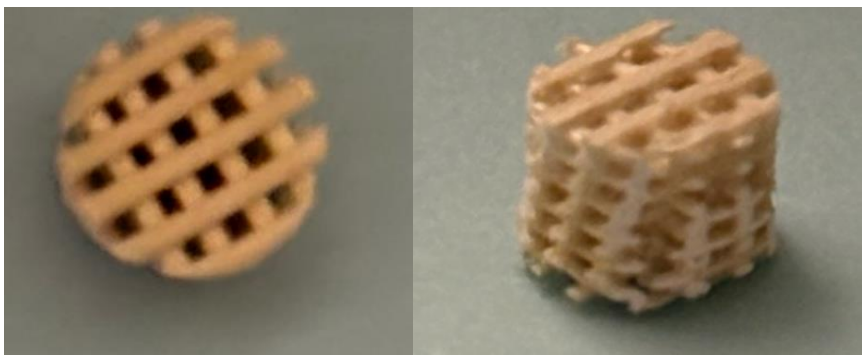

Figure 6. The constructed scaffold with the ability to be punched without significant deformation

handling, and repeated specimen preparation. These observations support the technical feasibility of the manufacturing concept under the conditions used. The main contribution of the study was procedural rather than biological. Both regions had the same nominal line width, spacing, and layer height; therefore, the scaffold was not architecturally graded by design. The regional distinction arose from composition: one region contained alginate and CMC, whereas the other contained alginate and a glass powder of nominal 45S5 composition. Sequential loading created a visually apparent transition during extrusion. Because that transition was not chemically or dimensionally characterized, the present findings establish gross continuity but not compositional gradient width, interfacial mixing, or interfacial strength. The CBCT workflow provided anatomical scale information. Root length showed the intended scaffold height, and the minimum measured canal diameter showed the lower range of specimen sizes. Nevertheless, the printed construct was a larger planar scaffold from which specimens were punched; it was not printed as a validated patient-specific intracanal implant. Direct seating, dimensional conformity, and canal occupancy were not measured. For this reason, the workflow should be interpreted as CBCT-informed rather than as evidence of CBCT-guided customization or root canal adaptation.

Alginate is widely used in hydrogel fabrication because it can undergo ionic gelation in the presence of calcium ions [13, 14]. CMC has been incorporated with alginate in printable dental tissue-engineering systems [10]. The addition of a nominal 45S5 glass component creates a second compositionally distinct formulation [11, 12]. However, the present study did not characterize the synthesized powder chemically or biologically and did not compare functional behavior between regions. Accordingly, no claims can be made regarding bioactivity, mineralization, cytocompatibility, degradation, or regenerative performance.

Macroscopic integrity after punching provides a practical handling observation but should not be interpreted as a mechanical test. The 50 punching procedures were nested within five completed scaffolds, and punch diameters were not treated as balanced comparison groups. Therefore, the findings do not demonstrate diameter-dependent resistance, mechanical strength, elastic behavior, or interfacial adhesion. Quantitative compression, tensile, shear, and interfacial testing would be required for those conclusions.

The feasibility finding should also be considered in light of one incomplete fabrication attempt. With only six attempts and no process-capability analysis, the study cannot provide a reliable manufacturing success rate. Future work should evaluate larger fabrication series and record extrusion pressure, material rheology, line-width fidelity, dimensional variation, and causes of printing failure. Such information would allow reproducibility and process robustness to be assessed.

This study used one modified extracted tooth as an anatomical reference, and the simulation did not represent a defined stage of immature root development. CBCT segmentation accuracy, resin-model accuracy, and scaffold-to-canal fit were not quantified. Actual printed filament dimensions, porosity, pore interconnectivity, swelling, and dimensional stability were not measured. The transition between formulations was evaluated visually only. The glass powder was used without quantitative particle-size, chemical, or phase characterization. Mechanical behavior, degradation, cytocompatibility, cell response, mineralization, antimicrobial effects, and in vivo performance were not investigated [16-18]. Finally, the small number of fabrication attempts and qualitative outcome assessment limit generalizability.

Future studies should evaluate printing fidelity using microscopy or micro-computed tomography, quantify the transition region, characterize the glass phase, test scaffold swelling and fit within anatomically relevant canal models, and assess mechanical and degradation behavior. Biological studies should then evaluate cytocompatibility, cell migration, vascular and odontogenic responses, and mineralization before translational conclusions are considered.

Conclusion

In this descriptive feasibility study, sequential extrusion through a single cartridge and nozzle produced a compositionally differentiated two-region hydrogel scaffold with preserved gross continuity in five of six fabrication attempts. The completed constructs remained macroscopically intact after crosslinking, washing, routine handling, and specimen preparation. These findings demonstrate fabrication feasibility only. CBCT-derived measurements served as anatomical references and did not establish root canal adaptation or patient-specific fit. Quantitative architectural, dimensional, mechanical, degradation, and biological validation is required before the functional or regenerative relevance of the approach can be determined.

Ethical Considerations

Compliance with ethical guidelines

This study was approved by the Research Ethics Committee of AJA University of Medical Sciences, Tehran, Iran (Code: IR.AJAUMS.REC.1405.044). Written informed consent was obtained for research use of the extracted tooth.

Funding

This study was extracted from the specialty thesis of Ali Shakibaei Fard, approved by the Department of Endodontics, Faculty of Dentistry, AJA University of Medical Sciences, Tehran, Iran.

Authors' contributions

Conceptualization, visualization, data curation, software, formal analysis, and validation: Mohammad Ali Ketabi and Ali Shakibaei Fard; Methodology and investigation: Mohammad Ali Ketabi, Arezoo Mirzaiy, Mohammad Reza Khodadadzadeh Khaledi, and Ali Shakibaei Fard; Writing the original draft: Mohammad Ali Ketabi; Review and editing: Mohammad Ali Ketabi, Arezoo Mirzaiy, Mohammad Reza Khodadadzadeh Khaledi, MohammadHossein Shahrezaee, and Ali Shakibaei Fard; Resources, supervision, project administration, and funding acquisition: Ali Shakibaei Fard.

Conflict of interest

The authors declared no conflict of interest.

Acknowledgments

The authors would like to thank the staff of the Department of Endodontics, Faculty of Dentistry, AJA University of Medical Sciences, Tehran, Iran, for their assistance during the experimental work.

References

[1] Huang GTJ. Apexification: the beginning of its end. International Endodontic Journal. 2009; 42(10):855-66. [DOI:10.1111/j.1365-2591.2009.01577.x] [PMID]

[2] Chala S, Abouqal R, Rida S. Apexification of immature teeth with calcium hydroxide or mineral trioxide aggregate: systematic review and meta-analysis. Oral Surgery, Oral Medicine, Oral Pathology, Oral Radiology, and Endodontics. 2011; 112(4):e36-42. [DOI:10.1016/j.tripleo.2011.03.047] [PMID]

[3] Lin JC, Lu JX, Zeng Q, Zhao W, Li WQ, Ling JQ. Comparison of mineral trioxide aggregate and calcium hydroxide for apexification of immature permanent teeth: A systematic review and meta-analysis. Journal of the Formosan Medical Associationc. 2016; 115(7):523-30. [DOI:10.1016/j.jfma.2016.01.010] [PMID]

[4] Hoque ME, Chuan YL, Pashby I. Extrusion based rapid prototyping technique: an advanced platform for tissue engineering scaffold fabrication. Biopolymers. 2012; 97(2):83-93. [DOI:10.1002/bip.21701] [PMID]

[5] Murphy SV, Atala A. 3D bioprinting of tissues and organs. Nature Biotechnology. 2014; 32(8):773-785. [DOI:10.1038/nbt.2958] [PMID]

[6] Borges CC, Estrela C, Decurcio DA, PÉcora JD, Sousa-Neto MD, Rossi-Fedele G. Cone-beam and micro-computed tomography for the assessment of root canal morphology: A systematic review. Brazilian Oral Research. 2020; 34:e056. [DOI:10.1590/1807-3107bor-2020.vol34.0056] [PMID]

[7] Diogenes A, Ruparel NB. Regenerative endodontic procedures: clinical outcomes. Dental Clinics of North America. 2017; 61(1):111-125. [DOI:10.1016/j.cden.2016.08.004] [PMID]

[8] Martin G, Ricucci D, Gibbs JL, Lin LM. Histological findings of revascularized/revitalized immature permanent molar with apical periodontitis using platelet-rich plasma. Journal of Endodontics. 2013;39(1):138-144. [DOI:10.1016/j.joen.2012.09.015] [PMID] [PMCID]

[9] Shimizu E, Jong G, Partridge N, Rosenberg PA, Lin LM. Histologic observation of a human immature permanent tooth with apical periodontitis after regenerative endodontic treatment. Journal of Endodontics. 2012; 38(9):1290-1294. [DOI:10.1016/j.joen.2012.06.017] [PMID]

[10] Mohabatpour F, Duan X, Yazdanpanah Z, Tabil XL, Lobanova L, Zhu N, et al. Bioprinting of alginate-carboxymethyl chitosan scaffolds for enamel tissue engineering in vitro. Biofabrication. 2023; 15(1):015009. [DOI:10.1088/1758-5090/acab35] [PMID]

[11] Rezabeigi E, Wood-Adams PM, Drew RA. Synthesis of 45S5 bioglass® via a straightforward organic, nitrate-free sol-gel process. Materials Science & Engineering. 2014; 40:248-52. [DOI:10.1016/j.msec.2014.03.042] [PMID]

[12] Rizwan M, Hamdi M, Basirun WJ. Bioglass® 45S5-based composites for bone tissue engineering and functional applications. Journal of Biomedical Materials Research. 2017; 105(11):3197-223. [DOI:10.1002/jbm.a.36194] [PMID]

[13] Kuo CK, Ma PX. Ionically crosslinked alginate hydrogels as scaffolds for tissue engineering: Part 1. Structure, gelation rate and mechanical properties. Biomaterials. 2001; 22(6):511-21. [DOI:10.1016/S0142-9612(00)00201-5] [PMID]

[14] Lee KY, Mooney DJ. Alginate: Properties and biomedical applications. Progress in Polymer Science. 2012;37(1):106-26. [DOI:10.1016/j.progpolymsci.2011.06.003] [PMID]

[15] Monfared MH, Ranjbar FE, Torbati M, Poursamar SA, Lotfibakhshaiesh N, Ai J, et al. Preparation and characterization of 3D nanocomposite scaffold from bioactive glass/β-tricalcium phosphate via robocasting method for bone tissue engineering. Journal of Non-Crystalline Solids. 2022; 593:121769. [DOI:10.1016/j.jnoncrysol.2022.121769]

[16] Hollister SJ. Porous scaffold design for tissue engineering. Nature Materials. 2005; 4(7):518-24. [DOI:10.1038/nmat1421] [PMID]

[17] Bose S, Vahabzadeh S, Bandyopadhyay A. Bone tissue engineering using 3D printing. Materials Today. 2013; 16(12):496-504. [DOI:10.1016/j.mattod.2013.11.017]

[18] Mirtabaei SM, Mollajavadi MY, Ketabi MA. The pore size effect on the degradation, tensile properties and cell viability of polycaprolactone/starch scaffold: Experimental study. Iranian Polymer Journal. 2025; 34(4):571-81. [DOI:10.1007/s13726-024-01397-4]